Journal of Theoretical and Applied Mechanics, Sofia, 2014, vol. 44, No. 4, pp. 51–68

DE GRUYTER
OPEN

DOI: 10.2478/jtam-2014-0022

INTERACTION BETWEEN A PERMEABLE CRACK AND PIEZOELECTRIC SCREW DISLOCATIONS, LINE FORCES AND LINE CHARGES IN A FINITE PIEZOELECTRIC CYLINDER*

H. P. Song, C. F. Gao

College of Aerospace Engineering,
State Key Laboratory of Mechanics and Control of Mechanical Structures,
Nanjing University of Aeronautics & Astronautics, Nanjing 210016, China,
e-mail: cfgao@nuaa.edu.cn

[Received 08 May 2014. Accepted 17 November 2014]

Abstract. The problem of a piezoelectric screw dislocation, line force and line charge around a permeable crack in a finite piezoelectric cylinder is dealt with in this paper. Utilizing the complex function and conformal mapping methods, the closed form solutions of the stress fields and the electric displacement fields are derived. The stress intensity factor and the image force are discussed in detail. The results show that the stress fields are in direct proportion to the line force, but independent of the line charge. The shielding effect produced by the dislocation increases with the increasing of the radius of the piezoelectric cylinder. Moreover, the unstable equilibrium point and the image force are also severely affected by the radius of the piezoelectric cylinder.
Key words: Screw dislocation, piezoelectric cylinder, crack, shielding effect, image force.

1. Introduction

Due to intrinsic coupling behaviour, piezoelectric materials are widely used in modern technology such as high power sonar transducers, electro-mechanical actuator, piezoelectric power supplies and micro-positioner. Hence, piezoelectric composites have become an important branch of modern engi-

*Corresponding author e-mail: cfgao@nuaa.edu.cn.

The work was supported by NSFC (No. 11232007 and 11202099), The Natural Science Foundation of Jiangsu Province (BK2011726), PAPD. Fundamental Research Funds for the Central Universities NS2012031 and the Open Fund of Zhejiang Provincial Top Key Discipline (zj1114).

neering materials with fast development of the intelligent characteristics of piezoelectric composite materials. However, defects are often unavoidable in such materials and affect the performance and reliability of the end products. Thus, in recent years, the study of piezoelectric materials with defects has received considerable interests. Pak [1] studied piezoelectric screw dislocations and derived the energy configuration force, a generalized Peach Koehler formula, acting on the dislocation. Liu et al. [2] derived the solution for a piezoelectric dislocation near an electrically impermeable elliptical cavity. Lee et al. [3] investigated the interaction between a piezoelectric screw dislocation and an electrically impermeable mode III crack of semi-infinite. Xiao et al [4] studied a dislocation emission mechanism for micro-crack initiation at the tip of a semi-infinite rigid line inhomogeneity in a piezoelectric solid. Wang et al [5] investigated a semi-infinite crack penetrating a piezoelectric circular inhomogeneity bonded to an infinite piezoelectric matrix through a linear viscous interface. Mousavi and Paavola [6] analyzed the cracked functionally graded piezoelectric strip. Song and Gao [7] studied the interaction between a screw dislocation, a rigid wedge inhomogeneity and an elastic circular inhomogeneity.

All the references above supposed that the normal component of the electric displacement could be treated as zero at the upper and lower crack faces. Jackson [8] proposed that the electric boundary conditions along an interface should be the continuity of the normal component of the electric displacement and the continuity of the tangent component of the electric field strength. Using such boundary conditions, Chen et al [9] discussed the difference of the mechanical and electrical fields produced by a line force, a line charge and a line screw dislocation under electrically impermeable and permeable boundary. Zhang [10-11] studied the crack width effect for piezoelectric materials, showing that the crack width has great influence on the crack growth because of the existence of electric field inside the crack. Kuna [12] discussed in detail the fracture mechanics of piezoelectric materials. Gross et al. [13–14] and Rangelov et al. [15] studied the crack problems in piezoelectric solids by boundary integral equation method.

However, the interaction of a piezoelectric screw dislocation with a permeable crack in a finite piezoelectric cylinder has not been studied, due to the complexity of the calculation. In the present paper, the problem of a piezoelectric screw dislocation, line force and line charge around a permeable crack in a finite piezoelectric cylinder is dealt with. The closed form solutions of the stress fields and the electric displacement fields are derived, utilizing the complex function and conformal mapping methods. The stress intensity factor and the image force are discussed in detail.

2. Problem statement and general treatment

Consider a transversely isotropic material belonging to the hexagonal crystal class 6 mm, the $x_1 - x_2$ plane is the isotropic basal plane, and the poling direction parallel to the x_3-axis. In contracted notation, the governing equations for the anti-plane strain problem (only out-of-plane displacements and in-plane electric fields) can be expressed as:

$$c_{44}\nabla^2 u_3 + e_{15}\nabla^2\phi = 0, \tag{1}$$

$$e_{15}\nabla^2 u_3 - \varepsilon_{11}\nabla^2\phi = 0, \tag{2}$$

where ∇^2 is the two-dimensional Laplacian operator, u_3 is the displacement in the x_3 direction and ϕ is the static electrical potential. c_{44}, e_{15} and ε_{11} are the elastic moduli, piezoelectric constant and the dielectric constant, respectively.

The governing field equations are given by:

$$\sigma_{13} = c_{44}\frac{\partial u_3}{\partial x_1} + e_{15}\frac{\partial \phi}{\partial x_1}, \tag{3}$$

$$\sigma_{23} = c_{44}\frac{\partial u_3}{\partial x_2} + e_{15}\frac{\partial \phi}{\partial x_2}, \tag{4}$$

$$D_1 = e_{15}\frac{\partial u_3}{\partial x_1} - \varepsilon_{11}\frac{\partial \phi}{\partial x_1}, \tag{5}$$

$$D_2 = e_{15}\frac{\partial u_3}{\partial x_2} - \varepsilon_{11}\frac{\partial \phi}{\partial x_2}. \tag{6}$$

Let u_3 and ϕ be the imaginary parts of the analytic complex functions:

$$u_3(x_1, x_2) = \operatorname{Im}\varphi_1(z), \quad \phi(x_1, x_2) = \operatorname{Im}\varphi_2(z), \quad z = x_1 + ix_2, \tag{7}$$

from Eq. (7), the constitutive equations can be represented as:

$$\sigma_{32} + i\sigma_{31} = C_{44}\varphi_1'(z) + e_{15}\varphi_2'(z), \tag{8}$$

$$D_2 + iD_1 = e_{15}\varphi_1'(z) - \varepsilon_{11}\varphi_2'(z). \tag{9}$$

and the electric field E, and the anti-plane shear strains γ, can be written as:

$$E_2 + iE_1 = -\varphi_2'(z), \quad \gamma_{32} + i\gamma_{31} = \varphi_1'(z). \tag{10}$$

Consider a finite piezoelectric cylinder containing a crack, the tip of the crack is at the center of the cylinder, a screw dislocation (b_z, b_ϕ), line force P and line charge Q are located at z_0, as shown in Fig. 1a.

For the current problem, the boundary conditions at the piezoelectric cylinder surface can be summarized as:

$$\sigma_\perp = 0, \quad D_\perp = 0, \tag{11}$$

where the subscript $\perp$ means perpendicular to the surface.

And the boundary conditions along the surface of the permeable crack have the form:

$$\sigma_\perp = 0, \quad D_\perp^+ = D_\perp^-, \quad E_\parallel^+ = E_\parallel^-, \tag{12}$$

where the subscript $\parallel$ means parallel to the surface.

Boundary conditions (11)–(12), can be written as:

$$\begin{aligned} &\mathrm{Im}[(e_{15}\phi_1'(z) - \varepsilon_{11}\phi_2'(z))e^{i\theta}] = 0, \quad \mathrm{Im}[(C_{44}\phi_1'(z) + e_{15}\phi_2'(z))e^{i\theta}] = 0, \\ &\mathrm{Re}[C_{44}\varphi_1'(z) + e_{15}\varphi_2'(z)] = 0, \qquad \mathrm{Im}[\varphi_2'(z)]^+ = \mathrm{Im}[\varphi_2'(z)]^-, \end{aligned} \tag{13}$$

$$\mathrm{Re}[e_{15}\varphi_1'(z) - \varepsilon_{11}\varphi_2'(z)]^+ = \mathrm{Re}[e_{15}\varphi_1'(z) - \varepsilon_{11}\varphi_2'(z)]^-. \tag{14}$$

The following transform function

$$w = \omega(z) = z^{1/2}, \quad z = G(w) = w^2, \tag{15}$$

which can map the half-plane with a half-circular inclusion (with radius $R' = R^{1/2}$) in the w-plane on to a cylinder (with radius R) with a crack in the z-plane (Fig. 1).

Consequently, the boundary conditions of eqs (13–14) may be represented as:

$$\mathrm{Im}\left[(e_{15}\phi_1'(w) - \varepsilon_{11}\phi_2'(w))\frac{dw}{dz}w^2\right] = 0,$$

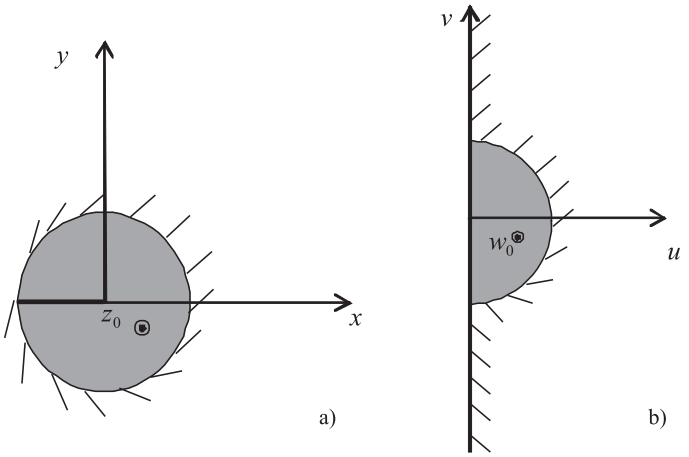

Fig. 1. a) A screw dislocation near a permeable crack in a finite piezoelectric cylinder; b) The w-plane

$$\mathrm{Im}\left[(C_{44}\phi_1'(w)+e_{15}\phi_2'(w))\frac{dw}{dz}w^2\right]=0, \quad \text{at } |w|=R',$$

$$\begin{aligned}&\mathrm{Re}\left[(C_{44}\varphi_1'(w)+e_{15}\varphi_2'(w))\frac{dw}{dz}\right]=0,\\ &\mathrm{Im}\left[\varphi_2'(w)\frac{dw}{dz}\right]^+=\mathrm{Im}\left[\varphi_2'(w)\frac{dw}{dz}\right]^-,\end{aligned} \tag{16}$$

$$\begin{aligned}&\mathrm{Re}[(e_{15}\varphi_1'(w)-\varepsilon_{11}\varphi_2'(w))\frac{dw}{dz}]^+\\ &\qquad=\mathrm{Re}[(e_{15}\varphi_1'(w)-\varepsilon_{11}\varphi_2'(w))\frac{dw}{dz}]^-, \text{ at } \mathrm{Re}[w]=0.\end{aligned} \tag{17}$$

Eqs.(16–17) can be further simplified to:

$$\mathrm{Im}[(e_{15}\phi_1'(w)-\varepsilon_{11}\phi_2'(w))w]=0, \text{ at } |w|=R', \tag{18-1}$$

$$\mathrm{Im}[(C_{44}\phi_1'(w)+e_{15}\phi_2'(w))w]=0, \text{ at } |w|=R', \tag{18-2}$$

$$\mathrm{Im}[C_{44}\varphi_1'(w)+e_{15}\varphi_2'(w)]=0, \text{ at } \mathrm{Re}[w]=0, \tag{19-1}$$

$$\mathrm{Re}[\varphi_2'(w)]^+ = -\,\mathrm{Re}[\varphi_2'(w)]^-, \text{ at } Re[w] = 0, \tag{19-2}$$

$$\mathrm{Im}[e_{15}\varphi_1'(w) - \varepsilon_{11}\varphi_2'(w)]^+ = -\,\mathrm{Im}[e_{15}\varphi_1'(w) - \varepsilon_{11}\varphi_2'(w)]^-, \quad \text{at } \mathrm{Re}[w] = 0, \tag{19-3}$$

where $w^+ = -w^-$ at $Re[w] = 0$.

3. A piezoelectric cylinder piezoelectric screw dislocation

The two complex potentials in the w plane can be expressed in the forms:

$$\phi_1'(w) = \frac{b_z}{2\pi}\frac{1}{w - w_0} + \phi_{10}'(w), \tag{20}$$

$$\phi_2'(w) = \frac{b_\phi}{2\pi}\frac{1}{w - w_0} + \phi_{20}'(w), \tag{21}$$

where $\phi_{10}'(w)$ and $\phi_{20}'(w)$ are holomorphic in the region $Re[w] \geq 0$ and $|w| \leq R'$.

In order to satisfy boundary condition (19-2), an image dislocation b_ϕ is put at $-w_0$, so $\phi_2'(w)$ can be expressed as:

$$\phi_2'(w) = \frac{b_\phi}{2\pi}\frac{1}{w - w_0} + \frac{b_\phi}{2\pi}\frac{1}{w + w_0}. \tag{22}$$

Similarly, two image dislocations with Burgers vector $-b_z - \dfrac{e_{15}}{c_{44}}b_\phi$ and $-\dfrac{e_{15}}{c_{44}}b_\phi$ are put at $-\overline{w}_0$ and $-w_0$ to satisfy boundary condition (19-1), thus we have:

$$\phi_1'(w) = \frac{b_z}{2\pi}\frac{1}{w - w_0} - \frac{c_{44}b_z + e_{15}b_\phi}{2\pi c_{44}}\frac{1}{w + \overline{w}_0} - \frac{e_{15}b_\phi}{2\pi c_{44}}\frac{1}{w + w_0}. \tag{23}$$

Luckily, solutions (22–23) also satisfy boundary condition (19-3). However, they dissatisfy boundary conditions (18-1) and (18-2).

The boundary conditions (18-1) and (18-2) are just the same as the problem of a screw dislocation inside a finite piezoelectric cylinder, which have been solved by Meguid and Deng [16].

$$\mathbf{\Phi'}_i(w) = \mathbf{B}\frac{1}{2\pi}\frac{1}{w - w_0} - \mathbf{B}\frac{1}{2\pi}\frac{1}{w - w^*}, \tag{24}$$

where $\mathbf{\Phi'}_i(w) = \left\{ \begin{array}{c} \phi_1'(w) \\ \phi_2'(w) \end{array} \right\}$, $\mathbf{B} = \left\{ \begin{array}{c} b_z \\ b_\varphi \end{array} \right\}$, $w^* = \dfrac{R'^2}{\overline{w}_0}$.

Eq. (24) can be seen as a screw dislocation with Burgers vector $\mathbf{B}$ located at w_0 and an image dislocation with Burgers vector $-\mathbf{B}$ located at w^*. Therefore, all the boundary conditions will be satisfied, if we make each dislocation in Eqs. (22–23) to have an image once again.

Accordingly, the final solutions are:

$$\phi_2'(w) = \frac{b_\phi}{2\pi}\frac{1}{w-w_0} + \frac{b_\phi}{2\pi}\frac{1}{w+w_0} - \frac{b_\phi}{2\pi}\frac{1}{w-w^*} - \frac{b_\phi}{2\pi}\frac{1}{w+w^*}, \tag{25}$$

$$\begin{aligned}\phi_1'(w) = {} & \frac{b_z}{2\pi}\frac{1}{w-w_0} - \frac{C_{44}b_z + e_{15}b_\phi}{2\pi C_{44}}\frac{1}{w+\overline{w}_0} - \frac{e_{15}b_\phi}{2\pi C_{44}}\frac{1}{w+w_0} \\ & - \frac{b_z}{2\pi}\frac{1}{w-w^*} + \frac{C_{44}b_z + e_{15}b_\varphi}{2\pi C_{44}}\frac{1}{w+\overline{w}^*} + \frac{e_{15}b_\varphi}{2\pi C_{44}}\frac{1}{w+w^*}.\end{aligned} \tag{26}$$

With the aid of the mapping function (15), the stress field at z due to a screw dislocation z_0 near a crack, can be obtained as:

$$\begin{aligned}\sigma_{32} + i\sigma_{31} &= C_{44}\varphi_1'(z) + e_{15}\varphi_2'(z) \\ &= \frac{C_{44}b_z + e_{15}b_\phi}{4\pi\sqrt{z}}\left[\frac{1}{w-w_0} - \frac{1}{w+\overline{w}_0} - \frac{1}{w-w^*} + \frac{1}{w+\overline{w}^*}\right],\end{aligned} \tag{27}$$

$$\begin{aligned}D_2 + iD_1 = e_{15}\phi_1'(z) - \varepsilon_{11}\phi_2'(z) = {} & \frac{e_{15}b_z - \varepsilon_{11}b_\phi}{4\pi\sqrt{z}}\left[\frac{1}{w-w_0} - \frac{1}{w-w^*}\right] \\ & - \frac{c_{44}e_{15}b_z + e_{15}^2 b_\phi}{4\pi\sqrt{z}C_{44}}\left[\frac{1}{w+\overline{w}_0} - \frac{1}{w+\overline{w}^*}\right] \\ & - \frac{e_{15}^2 b_\phi + C_{44}\varepsilon_{11}b_\phi}{4\pi\sqrt{z}C_{44}}\left[\frac{1}{w+w_0} - \frac{1}{w+w^*}\right].\end{aligned} \tag{28}$$

4. A line force and a line charge in the piezoelectric cylinder

Here, we ignore the intermediate steps, which are similar to the above section. The two analytic functions are

$$\phi_2'(w) = -\frac{e_{15}P + C_{44}Q}{2\pi(C_{44}\varepsilon_{11} + e_{15}^2)}\left[\frac{i}{w-w_0} + \frac{i}{w+w_0} + \frac{i}{w-w^*} + \frac{i}{w+w^*}\right], \tag{29}$$

$$\phi_1'(w) = -\frac{1}{2\pi(C_{44}\varepsilon_{11}+e_{15}^2)}\left[\frac{(\varepsilon_{11}P-e_{15}Q)i}{w-w_0}+\frac{(C_{44}\varepsilon_{11}+e_{15}^2)Pi}{C_{44}(w+\overline{w}_0)}\right.$$
$$-\frac{(e_{15}^2P+C_{44}e_{15}Q)i}{C_{44}(w+w_0)}+\frac{(\varepsilon_{11}P-e_{15}Q)i}{w-w^*}$$
$$\left.+\frac{(C_{44}\varepsilon_{11}+e_{15}^2)Pi}{C_{44}(w+\overline{w}^*)}-\frac{(e_{15}^2P+C_{44}e_{15}Q)i}{C_{44}(w+w^*)}\right]. \tag{30}$$

The stress field and the electric displacement field at z, can be obtained as:

$$\sigma_{32}+i\sigma_{31} = C_{44}\varphi_1'(z)+e_{15}\varphi_2'(z)$$
$$= -\frac{1}{4\sqrt{z}\pi}\left[\frac{Pi}{w-w_0}+\frac{Pi}{(w+\overline{w}_0)}+\frac{Pi}{w-w^*}+\frac{Pi}{(w+\overline{w}^*)}\right], \tag{31}$$

$$D_2+iD_1 = e_{15}\varphi_1'(z)-\varepsilon_{11}\varphi_2'(z) = -\frac{1}{4\sqrt{z}\pi}\left[-\frac{Qi}{w-w_0}+\frac{e_{15}Pi}{C_{44}(w+\overline{w}_0)}\right.$$
$$\left.-\frac{(e_{15}P+C_{44}Q)i}{C_{44}(w+w_0)}-\frac{Qi}{w-w^*}+\frac{e_{15}Pi}{C_{44}(w+\overline{w}^*)}-\frac{(e_{15}P+C_{44}Q)i}{C_{44}(w+w^*)}\right]. \tag{32}$$

Eq. (31) shows that the stress field is in direct proportion to the line force$P$, but independent of the line charge Q.

5. Impermeable crack solutions

Again, we ignore the intermediate steps, the two analytic functions of the impermeable crack are:

$$\phi_1'(w) = \frac{b_z}{2\pi}\left[\frac{1}{w-w_0}-\frac{1}{w+\overline{w}_0}-\frac{1}{w-w^*}+\frac{1}{w+\overline{w}^*}\right]$$
$$+\frac{e_{15}Q-\varepsilon_{11}P}{2\pi(C_{44}\varepsilon_{11}+e_{15}^2)}\left[\frac{i}{w-w_0}+\frac{i}{w+\overline{w}_0}+\frac{i}{w-w^*}+\frac{i}{w+\overline{w}^*}\right], \tag{33}$$

$$\phi_2'(w) = \frac{b_\phi}{2\pi}\left[\frac{1}{w-w_0}-\frac{1}{w+\overline{w}_0}-\frac{1}{w-w^*}+\frac{1}{w+\overline{w}^*}\right]$$
$$-\frac{C_{44}Q+e_{15}P}{2\pi(C_{44}\varepsilon_{11}+e_{15}^2)}\left[\frac{i}{w-w_0}+\frac{i}{w+\overline{w}_0}+\frac{i}{w-w^*}+\frac{i}{w+\overline{w}^*}\right]. \tag{34}$$

The stress field and electric displacement field at z can be obtained as:

$$\begin{aligned}(35)\quad \sigma_{32}+i\sigma_{31} &= C_{44}\varphi_1'(z)+e_{15}\varphi_2'(z)\\ &= \frac{C_{44}b_z+e_{15}b_\phi}{4\pi\sqrt{z}}\left[\frac{1}{w-w_0}-\frac{1}{w+\overline{w}_0}-\frac{1}{w-w^*}+\frac{1}{w+\overline{w}^*}\right]\\ &\quad -\frac{P}{4\pi\sqrt{z}}\left[\frac{i}{w-w_0}+\frac{i}{w+\overline{w}_0}+\frac{i}{w-w^*}+\frac{i}{w+\overline{w}^*}\right],\end{aligned}$$

$$\begin{aligned}(36)\quad D_2+iD_1 &= e_{15}\phi_1'(z)-\varepsilon_{11}\phi_2'(z)\\ &= \frac{e_{15}b_z-\varepsilon_{11}b_\phi}{4\pi\sqrt{z}}\left[\frac{1}{w-w_0}-\frac{1}{w+\overline{w}_0}-\frac{1}{w-w^*}+\frac{1}{w+\overline{w}^*}\right]\\ &\quad +\frac{Q}{4\pi\sqrt{z}}\left[\frac{i}{w-w_0}+\frac{i}{w+\overline{w}_0}+\frac{i}{w-w^*}+\frac{i}{w+\overline{w}^*}\right].\end{aligned}$$

6. Field intensity factors

The field intensity factors (FIFs) at the right tip of the crack can be obtained by:

$$(37)\qquad \mathbf{K}=\left[K^\sigma\ K^D\ K^\gamma\ K^E\right]^{\mathrm{T}}=\lim_{z\to 0}\sqrt{2\pi z}\left[\sigma_{32}\ D_2\ \gamma_{32}\ E_2\right]^{\mathrm{T}}.$$

Substituting Eqs. (27–28) and (31–32) into Eq. (37), yields:

$$\begin{aligned}(38)\quad K^\sigma = Re\Bigg[&-\frac{1}{2\sqrt{2\pi}}\left(-\frac{Pi}{w_0}+\frac{Pi}{\overline{w}_0}-\frac{Pi}{w^*}+\frac{Pi}{\overline{w}^*}\right)\\ &+\frac{C_{44}b_z+e_{15}b_\phi}{2\sqrt{2\pi}}\left(-\frac{1}{w_0}-\frac{1}{\overline{w}_0}+\frac{1}{w^*}+\frac{1}{\overline{w}^*}\right)\Bigg]\end{aligned}$$

$$\begin{aligned}(39)\quad K^D = Re\Bigg[&-\frac{1}{2\sqrt{2\pi}}\frac{e_{15}}{C_{44}}\left(\frac{Pi}{\overline{w}_0}-\frac{Pi}{w_0}+\frac{Pi}{\overline{w}^*}-\frac{Pi}{w^*}\right)\\ &+\frac{C_{44}e_{15}b_z+e_{15}^2b_\phi}{2\sqrt{2\pi}C_{44}}\left(-\frac{1}{w_0}-\frac{1}{\overline{w}_0}+\frac{1}{w^*}+\frac{1}{\overline{w}^*}\right)\Bigg]\end{aligned}$$

$$K^{\gamma} = Re\left[-\frac{1}{2\sqrt{2\pi}C_{44}}\left(-\frac{Pi}{w_0}+\frac{Pi}{\overline{w}_0}-\frac{Pi}{w^*}+\frac{Pi}{\overline{w}^*}\right)\right.$$
$$\left.+\frac{C_{44}b_z+e_{15}b_{\phi}}{2\sqrt{2\pi}C_{44}}\left(-\frac{1}{w_0}-\frac{1}{\overline{w}_0}+\frac{1}{w^*}+\frac{1}{\overline{w}^*}\right)\right] \tag{40}$$

$$K^{E} = 0. \tag{41}$$

Similarly, the FIFs at the right tip of the impermeable crack, are:

$$K^{\sigma} = Re\left[-\frac{1}{2\sqrt{2\pi}}\left(-\frac{Pi}{w_0}+\frac{Pi}{\overline{w}_0}-\frac{Pi}{w^*}+\frac{Pi}{\overline{w}^*}\right)\right.$$
$$\left.+\frac{C_{44}b_z+e_{15}b_{\phi}}{2\sqrt{2\pi}}\left(-\frac{1}{w_0}-\frac{1}{\overline{w}_0}+\frac{1}{w^*}+\frac{1}{\overline{w}^*}\right)\right], \tag{42}$$

$$K^{D} = Re\left[\frac{Q}{2\sqrt{2\pi}}\left(-\frac{i}{w_0}+\frac{i}{\overline{w}_0}-\frac{i}{w^*}+\frac{i}{\overline{w}^*}\right)\right.$$
$$\left.+\frac{e_{15}b_z-\varepsilon_{11}b_{\phi}}{2\sqrt{2\pi}}\left(-\frac{1}{w_0}-\frac{1}{\overline{w}_0}+\frac{1}{w^*}+\frac{1}{\overline{w}^*}\right)\right], \tag{43}$$

$$K^{\gamma} = Re\left[\frac{e_{15}Q-\varepsilon_{11}P}{2\sqrt{2\pi}(C_{44}\varepsilon_{11}+e_{15}^2)}\left(-\frac{i}{w_0}+\frac{i}{\overline{w}_0}-\frac{i}{w^*}+\frac{i}{\overline{w}^*}\right)\right.$$
$$\left.+\frac{b_z}{2\sqrt{2\pi}}\left(-\frac{1}{w_0}-\frac{1}{\overline{w}_0}+\frac{1}{w^*}+\frac{1}{\overline{w}^*}\right)\right], \tag{44}$$

$$K^{E} = Re\left[\frac{C_{44}Q+e_{15}P}{2\sqrt{2\pi}(C_{44}\varepsilon_{11}+e_{15}^2)}\left(-\frac{i}{w_0}+\frac{i}{\overline{w}_0}-\frac{i}{w^*}+\frac{i}{\overline{w}^*}\right)\right.$$
$$\left.-\frac{b_{\phi}}{2\sqrt{2\pi}}\left(-\frac{1}{w_0}-\frac{1}{\overline{w}_0}+\frac{1}{w^*}+\frac{1}{\overline{w}^*}\right)\right]. \tag{45}$$

Eqs. (38) and (42) show that the stress intensity factors of the two cases are identical and in direct proportion to the P and $C_{44}b_z + e_{15}b_{\phi}$. $K^{\gamma}$of the impermeable crack is in direct proportion to b_z, but independent of b_{ϕ}. $K^{E}$of the impermeable crack is in direct proportion to b_{ϕ}, but independent of

b_z. $K^\gamma$of the permeable crack is in direct proportion to $\dfrac{C_{44}b_z + e_{15}b_\phi}{C_{44}}$. K^E of the permeable crack is zero.

It is worth to point out, that there exists a "limited permeable crack" in the literature. The boundary conditions of the limited permeable crack are relatively complicated, so it is very difficult to obtain analytical solutions. But, we know that the solution of the limited permeable crack generally lies between the solution of the permeable crack and the solution of the impermeable crack, and the limited permeable crack can reduce to permeable crack or impermeable crack, under certain situations.

Assuming that the piezoelectric ceramic is PZT-5H, and its electroelastic properties are:

$$C_{44} = 2.3 \times 10^{10} N/m^2, \quad e_{15} = 17 C/m^2, \quad \varepsilon_{11} = 150.4 \times 10^{-10} C/Vm.$$

Eq. (28) shows that the stress intensity factor and electric displacement factor produced by the dislocation is in direct proportion to $C_{44}b_z + e_{15}b_\phi$. Which means, if $C_{44}b_z + e_{15}b_\phi = 0$, namely $\dfrac{b_\phi}{b_z} = -\dfrac{C_{44}}{e_{15}}$, the dislocation produce no stress intensity factor at all. And the stress intensity factor and the electric displacement factor are independent of the line charge Q.

The stresses intensity factor (SIF) produced by the line force for different values of R, as a function of θ, is shown in Fig. 2. It is seen that when $-\pi < \theta < 0$, the stresses intensity factor produced by the line force is negative. While the stresses intensity factor, produced by the line force is positive, if $0 < \theta < \pi$. The absolute value of the stresses intensity factor decreases with the value of R increasing. Which means, a smaller piezoelectric cylinder is more likely to fracture.

The curves for variations of SIF produced by the dislocation with respect to θ with different values of R, are shown in Fig. 3. It is found, that the SIF produced by the dislocation is negative (shielding effect). The shielding effect increases with increasing of R. Which means, the dislocation produces less shielding effect in smaller piezoelectric cylinders.

The normalized stresses intensity factor (SIF) as a function of R, is shown in Fig. 4. It is seen, that the dislocation in piezoelectric cylinder produces stronger shielding effect. And the stresses intensity factor, produced by the line force, is independent of the material parameters of the piezoelectric cylinder.

The displacement intensity factor K^D, as a function of b_ϕ, is shown in Fig. 5. It is seen that $K^D$of permeable crack decreases with increasing of b_ϕ. But $K^D$of impermeable crack increases with increasing of b_ϕ.

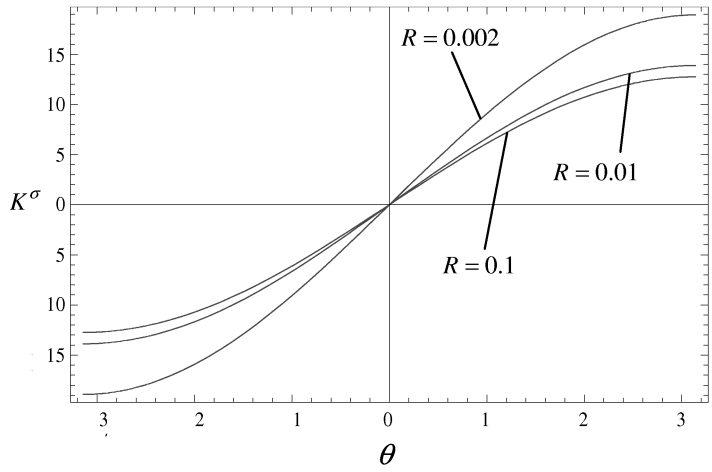

Fig. 2. Curves for SIF K^σ versus θ with different value of R at $b_z = b_\varphi = 0$, $P = 1N$, $d = 0.001m$

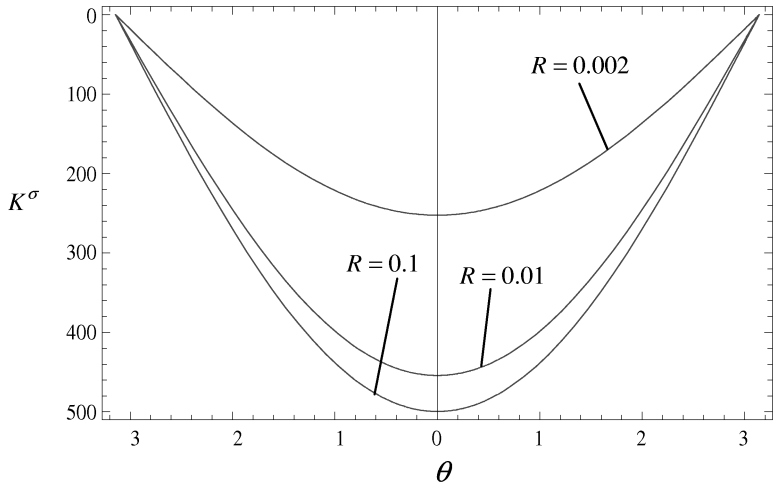

Fig. 3. Curves for SIF K^σ versus θ with different value of R at $b_z = 10^{-9}m$, $b_\varphi = 1V$, $P = 0$, $d = 0.001m$

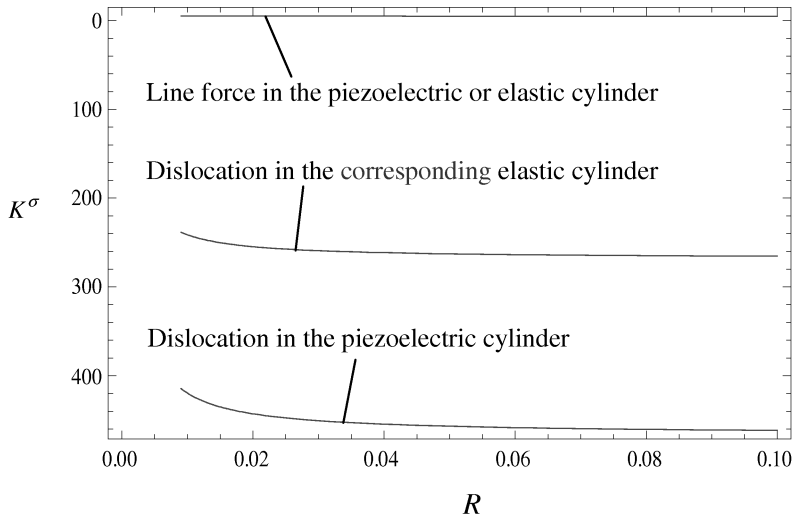

Fig. 4. Curves for SIF K^σ versus R at $b_z = 10^{-9}m$, $b_\varphi = 1V$, $P = 1N$, $d = 0.001m$, $\theta = \pi/4$

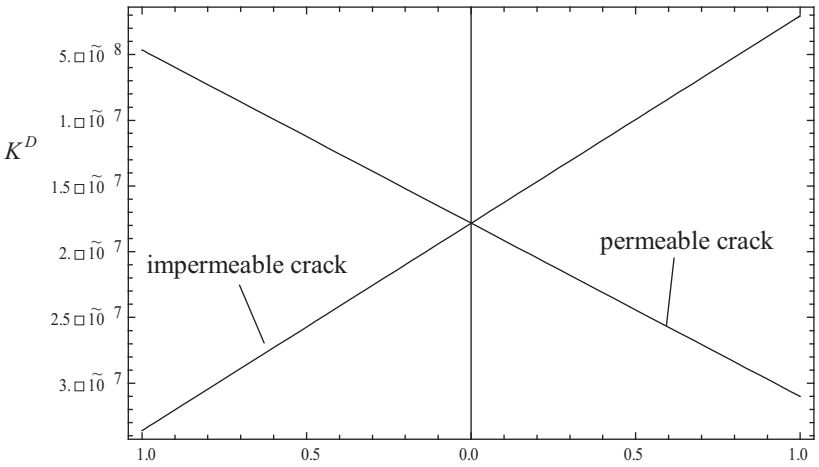

Fig. 5. Curves for SIF K^D versus b_φ at $b_z = 10^{-9}m$, $P = Q = 0$, $d = 0.001m$, $R = 0.01m$, $\theta = \pi/4$

6. Image force

The generalized Peach-Koehler forces are [17]:

$$F_1 = b_x\tilde{\sigma}_{12} + b_y\tilde{\sigma}_{22} + b_z\tilde{\sigma}_{23} - b_\varphi\tilde{D}_2, \tag{46}$$

$$F_2 = -b_x\tilde{\sigma}_{11} - b_y\tilde{\sigma}_{12} - b_z\tilde{\sigma}_{13} + b_\varphi\tilde{D}_1. \tag{47}$$

The image force acting on the screw dislocation can be written as:

$$F_{imag} = F_1 - iF_2 = b_z[\tilde{\sigma}_{32}(z_0) + i\tilde{\sigma}_{31}(z_0)] - b_\varphi[\tilde{D}_2(z_0) + i\tilde{D}_1(z_0)], \tag{48}$$

where $\tilde{\sigma}_{13}(z_0)$ and $\tilde{\sigma}_{23}(z_0)$ are the components of the perturbation stress, and $\tilde{D}_1(z_0)$ and $\tilde{D}_2(z_0)$ are the components of the perturbation electric displacement.

For the case of $P = Q = 0$, the image force of a dislocation near a permeable crack can be expressed as:

$$\begin{aligned} F_{imag} = {} & \frac{C_{44}b_z^2 + e_{15}b_zb_\varphi}{4\pi w_0}\left(-\frac{1}{2w_0} - \frac{1}{w_0+\overline{w}_0} - \frac{1}{w_0-w^*} + \frac{1}{w_0+\overline{w}^*}\right) \\ & - \frac{e_{15}b_zb_\varphi - \varepsilon_{11}b_\varphi^2}{4\pi w_0}\left(-\frac{1}{2w_0} - \frac{1}{w_0-w^*}\right) \\ & + \frac{C_{44}e_{15}b_zb_\varphi + e_{15}^2b_\varphi^2}{4\pi w_0 C_{44}}\left(\frac{1}{w_0+\overline{w}_0} - \frac{1}{w_0+\overline{w}^*}\right) \\ & + \frac{e_{15}^2b_\varphi^2 + C_{44}\varepsilon_{11}b_\varphi^2}{4\pi w_0 C_{44}}\left(\frac{1}{2w_0} - \frac{1}{w_0+w^*}\right). \end{aligned} \tag{49}$$

Accordingly, the image force of a dislocation near a impermeable crack is:

$$F_{imag} = \frac{C_{44}b_z^2 + \varepsilon_{11}b_\phi^2}{4\pi w_0}\left(-\frac{1}{2w_0} - \frac{1}{w_0+\overline{w}_0} - \frac{1}{w_0-w^*} + \frac{1}{w_0+\overline{w}^*}\right). \tag{50}$$

The same as the above section, we assuming that the material is PZT-5H, and letting the dislocation to lie on the x-axis. Fig. 6 shows the normalized image force $F_x/C_{44}b_z^2$ versus R. It is seen, that the value of $F_x/C_{44}b_z^2$ is always negative, which means the crack attracts the dislocation. The dislocation inside the piezoelectric cylinder suffers weaker attraction. The attraction force increases with the value of R increasing.

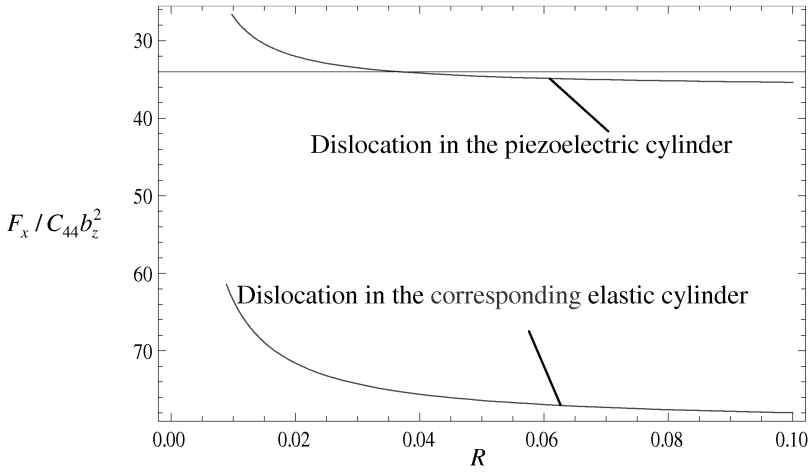

Fig. 6. Curves for normalized image force $F_x/C_{44}b_z^2$ versus R at $b_z = 10^{-9}m$, $b_\varphi = 1V$, $R = 0.01m$, $\theta = 0$

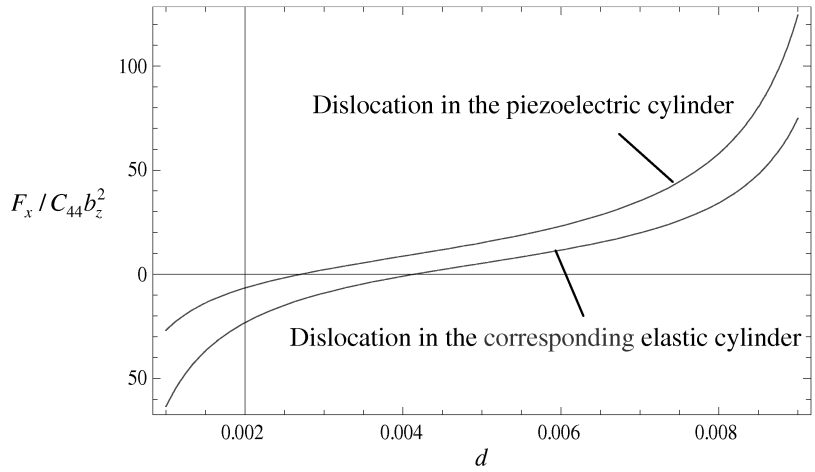

Fig. 7. Curves for normalized image force $F_x/C_{44}b_z^2$ versus d at $b_z = 10^{-9}m$, $b_\varphi = 1V$, $d = 0.0001m$, $\theta = 0$

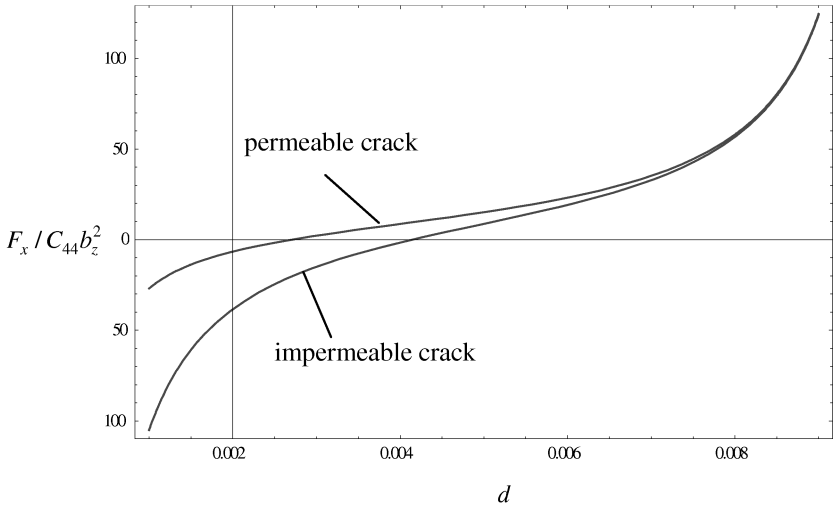

Fig. 8. Curves for normalized image force $F_x/C_{44}b_z^2$ versus d at $b_z = 10^{-9}m$, $b_\varphi = 1V$, $R = 0.01m$, $\theta = 0$

The curves for variations of normalized image force $F_x/C_{44}b_z^2$, with respect to the distance between the dislocation and the crack tip d, are shown in Fig. 7. It is found, that the value of $F_x/C_{44}b_z^2$ is negative at first, and become positive with the value of d increasing. Therefore, there is an unstable equilibrium point in the x-axis. The free surface attracts the dislocation. And the dislocation inside the piezoelectric cylinder suffers stronger attraction.

The normalized image force $F_x/C_{44}b_z^2$, as a function of d, is shown in Fig. 8. It is seen, that the dislocation near an impermeable crack suffers stronger attraction. And the normalized image forces of the two cases tend to be identical, when the dislocation is away from the crack.

7. Conclusions

The problem of a piezoelectric screw dislocation, line force and line charge around a permeable crack in a finite piezoelectric cylinder is dealt with in this paper. The closed form solutions of the stress fields and the electric displacement fields are derived, utilizing the complex function and conformal mapping methods. The stress intensity factor and the image force are discussed in detail. In summary, the following conclusions can be obtained:

(1) The stress field is in direct proportion to the line force P, but independent of the line charge Q.

(2) The absolute value of the stresses intensity factor produced by the line force decreases with the value of R increasing. While the shielding effect produced by the dislocation increases with the increasing of R. Which means, a smaller piezoelectric cylinder is more likely to fracture.

(3) The dislocation in piezoelectric cylinder produces stronger shielding effect. And the stresses intensity factor produced by the line force is independent of the material parameters of the piezoelectric cylinder.

(4) There is an unstable equilibrium point in the x-axis. The free surface attracts the dislocation. And compared with the elastic material situation, the dislocation inside the piezoelectric cylinder suffers stronger attraction.

REFERENCES

[1] Pak, Y. E. Force on a Piezoelectric Screw Dislocation. *J. Appl. Mech.,* **57** (1990), 863–869.

[2] Liu, J. X., B. Wang, S. Y. Du. Line Force, Charge and Dislocation in Anisotropic Piezoelectric Materials with an Elliptic Hole or a Crack. *Mech. Res. Commun.*, **24** (1997), 399–405.

[3] Lee, K. Y., W. G. Lee, Y. E. Pak. Interaction Between a Semi-infinite Crack and a Screw Dislocation in a Piezoelectric Material. *ASME J. Appl. Mech.*, **67** (2000), 165–170.

[4] Xiao, Z. M., H. X. Zhang, B. J. Chen. Micro-crack Initiation at the Tip of a Semi-infinite Rigid Line Inhomogeneity in Piezoelectric Solids. *In. J. Eng Sci.,* **43** (2005), 1223–1233.

[5] Wang, X., E. Pan, P. W. Chung. On a Semi-infinite Crack Penetrating a Piezoelectric Circular Inhomogeneity with a Viscous Interface. *Int. J. Solids Structures*, **46** (2009), 203–216.

[6] Mousavi, S. M., J. Paavola. Analysis of Cracked Functionally Graded Piezoelectric Strip. *Int. J. Solids Structures*, **50** (2013), 2449–2456.

[7] Song, H. P., C. F. Gao. The Interaction Between a Screw Dislocation and a Rigid Wedge Inhomogeneity with an Elastic Circular Inhomogeneity at the Tip. *Meccanica*, **47** (2012), 1097–1102.

[8] Jackson, J. D. Classical Electrodynamics, New York, John Wiley, 1976.

[9] Chen, B. J., Z. M. Xiao, K. M. Liew. A Screw Dislocation Interacting with a Finite Crack in a Piezoelectric Medium. *Int. J. Eng. Sci.,* **42** (2004), 1325–1345.

[10] Zhang, T. Y. Effect of Sample Width on the Energy Release Rate and Electric Boundary Conditions along Crack Surfaces in Piezoelectric Materials. *Int. J. Fract.,* **66** (1994), R33–R38.

[11] Zhang, T. Y. Fracture Mechanics for a Mode III Crack in a Piezoelectric Material. *Int. J. Solids Structures*, **33** (1996), 343–359.

[12] Kuna, M. Fracture Mechanics of Piezoelectric Materials–where are We Right Now. *Eng. Fract. Mech.,* **77** (2010), 309–326.

[13] Rangelov, T., P. Dineva, D. Gross. Effect of Material Inhomogeneity on the Dynamic Behaviour of Cracked Piezoelectric Solids: A BIEM Approach. *ZAMM – Z. Angew. Math. Mech.*, **88** (2008), No. 2, 86–99.

[14] Gross, D., P. Dineva, T. Rangelov. BIEM Solution of Piezoelectric Cracked Finite Solids under Time-Harmonic Loading. *Eng. Anal. Bound. Elem.*, **31** (2007), No. 2, 152–162.

[15] Rangelov, T., M. Marinov, P. Dineva. Time-harmonik Behaviour of Cracked Piezoelectric Solid by Boundary Integral Equation Method. *Journal of Theoretical and Applied Mechanics*, **44** (2014), No. 1, 55–78.

[16] Meguid, M. A., W. Deng. Electro-elastic Interaction between a Screw Dislocation and an Elliptical Inhomogeneity in Piezoelectric Materials. *Int. J. Solids Structures*, **35** (1997), 1467–1482.

[17] Song, H. P., C. F. Gao. Interaction of a Piezoelectric Screw Dislocation with a Blunt Mode III Crack in a Piezoelectric Material. *Engineering Fracture Mechanics*, **96** (2012), 687–700.